

# Dependence of Particle Initiated PD Characteristics on Size and Position of Metallic Particle Adhering to the Spacer Surface in GIS

F. N. Budiman, Y. Khan, A. A. Khan, A. Beroual, N. H. Malik, and A. A. Al-Arainy

**Abstract**—It is well known that metallic particles reduce the reliability of Gas-Insulated Substation (GIS) equipments by initiating partial discharge (PDs) that can lead to breakdown and complete failure of GIS. This paper investigates the characteristics of PDs caused by metallic particle adhering to the solid spacer. The PD detection and measurement were carried out by using IEC 60270 method with particles of different sizes and at different positions on the spacer surface. The results show that a particle of certain size at certain position possesses a unique PD characteristic as compared to those caused by particles of different sizes and/or at different positions. Therefore PD characteristics may be useful for the particle size and position identification.

**Keywords**—Particle, partial discharge, GIS, spacer.

## I. INTRODUCTION

THE use of SF<sub>6</sub> in power industry and especially in GIS has received a wide acceptance around the world due to the advantages this gas presents, including high dielectric strength, compactness, maintenance free nature, non-toxicity and non-flammability as well as good arc quenching properties [1-3].

However, the presence of metallic particles, which may be introduced in GIS equipments during manufacture, installation, and/or operation can deteriorate the reliability of GIS. Indeed, when a free metallic particle reaches the vicinity of spacer near the triple junction, it can easily adhere to the spacer surface then disturbing the distribution of the electric field around the spacer. The enhancement of local electric field at this particle leads to the initiation of PDs around the triple junction resulting thence in the system malfunction [4-7].

As the severity and the pattern of such PDs are determined

This work is sponsored by National Plan for Science and Technology, King Saud University Riyadh, Saudi Arabia, through research project # 08-ENE216-02.

F.N. Budiman, Y. Khan, A. A. Khan, N. H. Malik, and A. A. Al-Arainy are with Saudi Aramco Chair in Electrical Power, Electrical Engineering Department, College of Engineering, King Saud University, Riyadh, Saudi Arabia.

A. Beroual is with Ecole Centrale de Lyon, University of Lyon, AMPERE Lab CNRS UMR 5005, 36 avenue Guy de Collongue, Ecully, France and is Visiting Professor at Saudi Aramco Chair in Electrical Power, King Saud University, Riyadh, Saudi Arabia.

**Corresponding Author:** Y. Khan, Electrical Engineering Department, King Saud University, Riyadh 11421 Saudi Arabia (Phone: +966 1 4679813; fax: +966 1 4676140; e-mail: yasink@ksu.edu.sa).

by the particle dimensions and position on the spacer surface [8]-[10], it is necessary to identify the PD signals generated by particles of different sizes and at different positions.

This study is intended to investigate the dependence of PDs characteristics on the size and the position of particle adhering to the spacer surface in GIS. It is expected that the obtained results can be used to distinguish and estimate various particle sizes and positions on the spacer surface.

## II. EXPERIMENTAL SETUP AND METHOD

The system studied is SF<sub>6</sub>-filled GIS chamber containing a parallel-plane electrodes arrangement with an inserted Perspex (Plexiglas) cylindrical spacer. For creating the defect, a cylindrical stainless-steel contaminating particle of 0.5 mm diameter was attached to the spacer surface. As shown in Fig. 1, the particle size (length) is denoted as  $L$ , while the particle position is defined by  $H$ , which is the distance between the bottom tip of the particle and the grounded electrode.

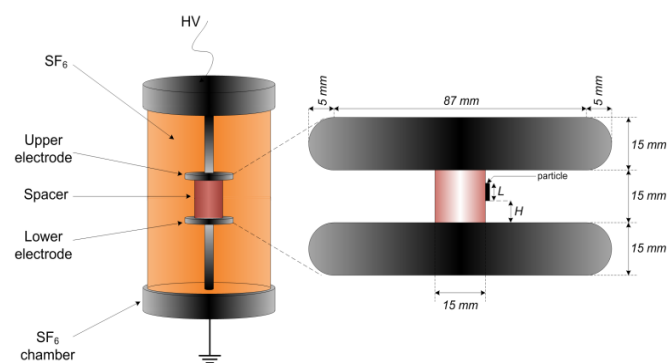


Fig. 1 The studied GIS chamber with the enlarged shape of the electrode-spacer system.

The PD measurements were performed by using IEC 60270 method [11], as shown in Fig. 2(a); and the PDs signal acquisition was carried out by using Hipotronics Digital PD Acquisition System. The employed system is able to detect PDs signals with sensitivity of less than 5 pC and phase resolution of 0.35 degrees. For measurements, the bandwidth of the PDs detection instrument was set at a lower limit of 20 kHz and an upper limit of 300 kHz. The calibration process is automated and once accomplished, the system calculates and displays a noise floor and allows amplifier ranges to be changed without affecting the system calibration in any way.

The components of the experimental setup are shown in Fig. 2(b).

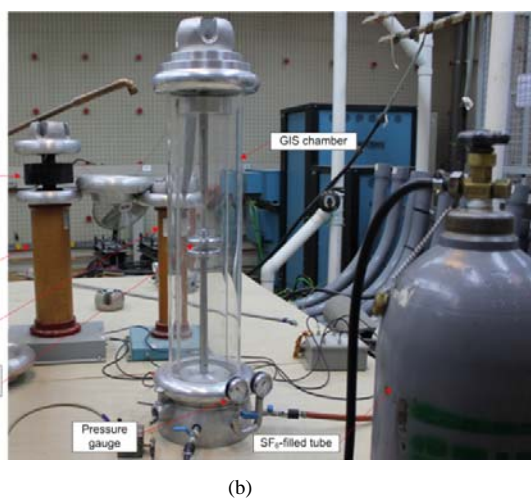
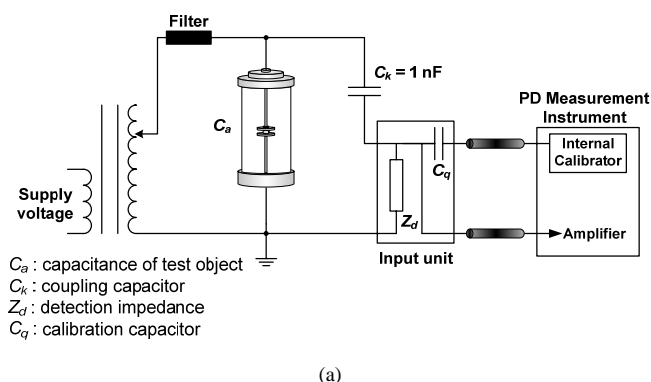


Fig. 2 (a) Schematic diagram based on IEC 60270 standard PD measurement setup used in the study (b) The components

To analyze the effect of the particle size and position, particle of 2 mm and 3 mm lengths were placed at various positions on the spacer surface. The particle adhered to the spacer of following positions: (a) gap center; (b) in contact with the upper (HV) electrode; (c) in contact with the grounded electrode; (d) between gap center and the HV electrode; and (e) between gap center and the grounded electrode. These positions are illustrated in Fig. 3 and are labeled as  $P_1$ ,  $P_2$ ,  $P_3$ ,  $P_4$ , and  $P_5$ . The values of  $H$  for  $P_1$  to  $P_5$  are listed in Table I.

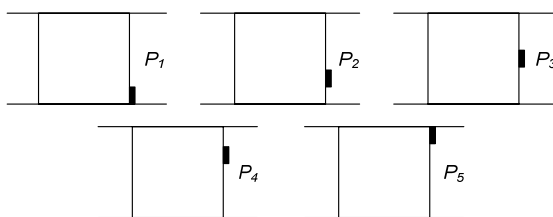


Fig. 3 Various particle positions on the spacer surface used in the study

TABLE I  
THE VALUES OF  $H$  FOR VARIOUS PARTICLE POSITIONS

Particle Position	The distance between particle and grounded electrode $H$ (mm)	
	For particle of 2mm length	For particle of 3mm length
$P_1$	0	0
$P_2$	3.25	3
$P_3$	6.5	6
$P_4$	9.75	9
$P_5$	13	12

A 100kV, 60 Hz, AC high voltage power supply was used. The voltage was increased gradually at a step of  $\sim 0.5$ kV till the PD inception was noted. In this study,  $\text{SF}_6$  pressures used were 1, 1.5, 2, 2.5, and 3 bars.

The PD inception voltage (PDIV) values for all particle sizes and positions are shown in Fig. 4. It is found that the PDIV values at various  $\text{SF}_6$  pressures are very close each other. The values given in Fig. 4 are the average values of PDIVs obtained at all  $\text{SF}_6$  pressures. Fig. 4 shows that PDIV values depend on the particle size and position. However, they lie in a close range.

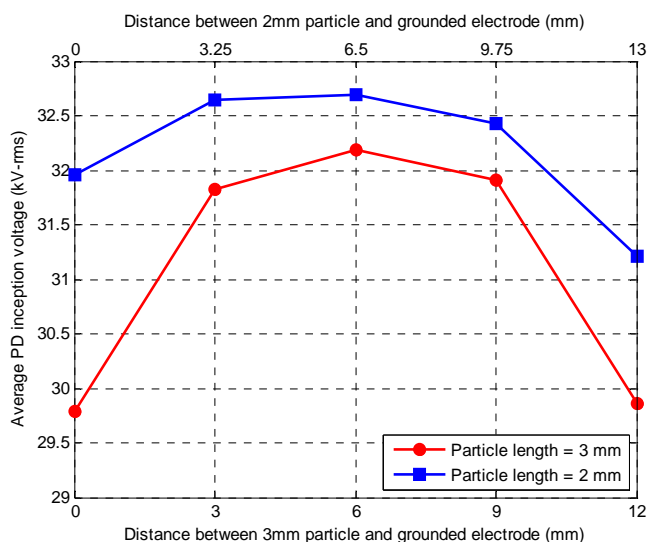


Fig. 4 PD inception voltages for all particle sizes (lengths) and positions.

For comparing the PD pulse characteristics due to particles of different sizes and at different positions, the same voltage was applied for all cases. In this study, 35 kV<sub>rms</sub> AC voltage was chosen, as this value is above the PDIV values for all cases. The measurement results for each case were acquired from the PD detection equipment in the form of data file containing data of every single recorded PD pulse. These data were further processed by using PD data processing application developed by using MATLAB version R2010a.

### III. RESULTS AND DISCUSSIONS

In this section, PD characteristics are discussed along with their dependence on the particle size and position as well as on  $\text{SF}_6$  pressure.

**A. Effect of Particle Size (length) on PD Characteristics**

The effect of particle length was investigated by examining the total PD magnitude in each case. The total PD magnitude was calculated during PD acquisition of 10 blocks using the following expression;

$$\text{Total PD magnitude} = \sum_{i=1}^n |q_i| \quad (1)$$

where  $q_i$  is the magnitude of individual PD pulse (in pC) and  $n$  is the number of acquired PD pulses in each case.

The total PD magnitude for both particle lengths, i.e. 2 mm and 3 mm, obtained at 1 bar and 3 bar SF<sub>6</sub> pressures is shown in Fig. 5. It is shown in Fig. 5(a) that at lower SF<sub>6</sub> pressure, i.e. 1 bar, 3 mm, particle generates higher PD magnitude than 2 mm particle. The difference in the total PD magnitude is minimum when the particle is at the gap center. Meanwhile, at higher SF<sub>6</sub> pressure (Fig. 5(b)), the condition of particle adhering in the gap center gives the lowest difference between the total PD magnitudes of both particles. Moreover, the average difference is also lower at higher SF<sub>6</sub> pressure.

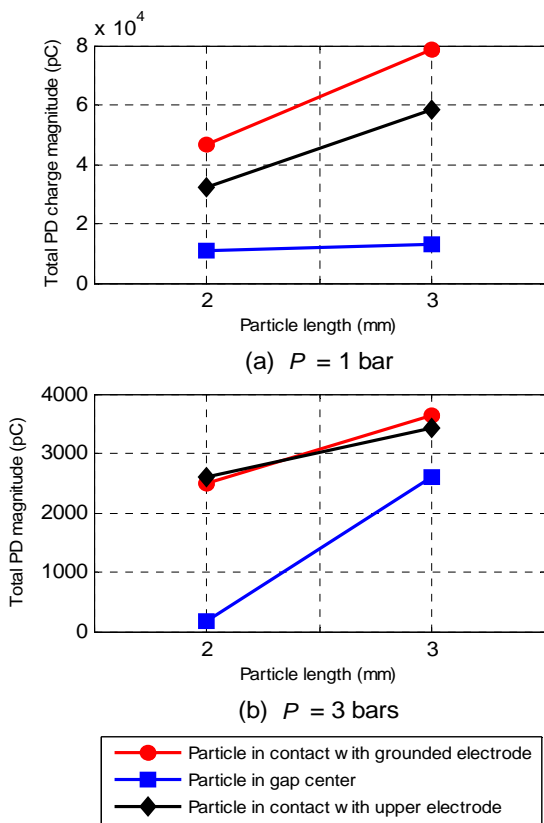


Fig. 5 The total PD magnitude for all particle lengths

**B. Effect of Particle Position on PD Characteristics**

To investigate the dependence of PD characteristics on the particle position on the spacer surface, the PRPD ( $\phi$ - $q$  characteristic) pattern for each particle position was established. The results for 3 mm particle at 2.5 bar SF<sub>6</sub> pressure are shown in Fig. 6. They are obtained from 10 s PD

acquisition. The relationship between particle position and PD pattern can be characterized by comparing the total PD magnitude occurring in the positive half-cycle with that occurring in the negative half-cycle. Referring to Fig. 6, when the particle is in contact with the grounded electrode (i.e.  $H = 0$  mm), PD occurring in the negative half-cycle has a higher total magnitude. Meanwhile, the ratio between the total PD magnitude in the negative half-cycle and the total PD magnitude in the positive half-cycle becomes lower when the particle is located between the lower electrode and the gap center, i.e.  $H = 3.25$  mm. As the particle location is shifted towards the upper electrode, the PD total magnitude in the positive half-cycle becomes higher as compared to that in the negative half-cycle.

Such a relationship is further depicted in Table II. Table II shows more clearly the effect of particle position by presenting the percentage of the total PD magnitude in each half-cycle of the applied voltage at 2.5 bar SF<sub>6</sub> pressure. When the particle is below the gap center, a higher PD magnitude occurs in the negative half-cycle. When the particle touches the grounded electrode, the highest percentage, i.e. 80.4%, is achieved. Conversely, PD with a higher magnitude in the positive half-cycle is obtained when the particle adheres to the spacer above the gap center. In case of the contact between the particle and the HV electrode, the highest percentage is achieved, which is 68.45%. When the particle is placed at the gap center, the total PD magnitude in the positive half-cycle is slightly higher than that in the negative half-cycle. However, the ratio is lower when compared to the other cases, i.e. when the particle is other than at the gap center.

Similar pattern is also obtained with the same particle length, but at a higher SF<sub>6</sub> pressure, i.e. 3 bars. As presented in Table III, the highest and the lowest values of the ratio between total PD magnitudes in the negative half-cycle and in the positive half-cycle are also met when the particle are in contact with the grounded electrode and with the HV electrode, respectively. However, the variation of such a ratio is lower when the particle is not in contact with the electrode. Consequently, it is slightly more difficult to differentiate the particle position under these conditions.

**C. Effect of SF<sub>6</sub> Pressure on PD Characteristics**

The effect of SF<sub>6</sub> pressure on PD characteristics is examined by comparing the total PD magnitude at all pressures. The results for both particle lengths (2 mm and 3 mm) at all positions obtained from 10 s PD acquisition are shown in Fig. 7.

Fig. 7(a) shows that at 1 bar, PDs with high total magnitude occur around the particle. When the pressure is increased to 1.5 bars, the total PD magnitude drastically decreases up to much lower values. Meanwhile, when the pressure is further increased up to 2.5 bars, the decrease in the total PD magnitude is very low. Thus, the curve looks almost pure horizontal from  $P = 1.5$  to  $P = 2.5$  bars, except when the particle is in contact with the grounded electrode. A slight different finding is obtained when the SF<sub>6</sub> pressure is increased from 2.5 to 3 bars. There is an obvious decrease in

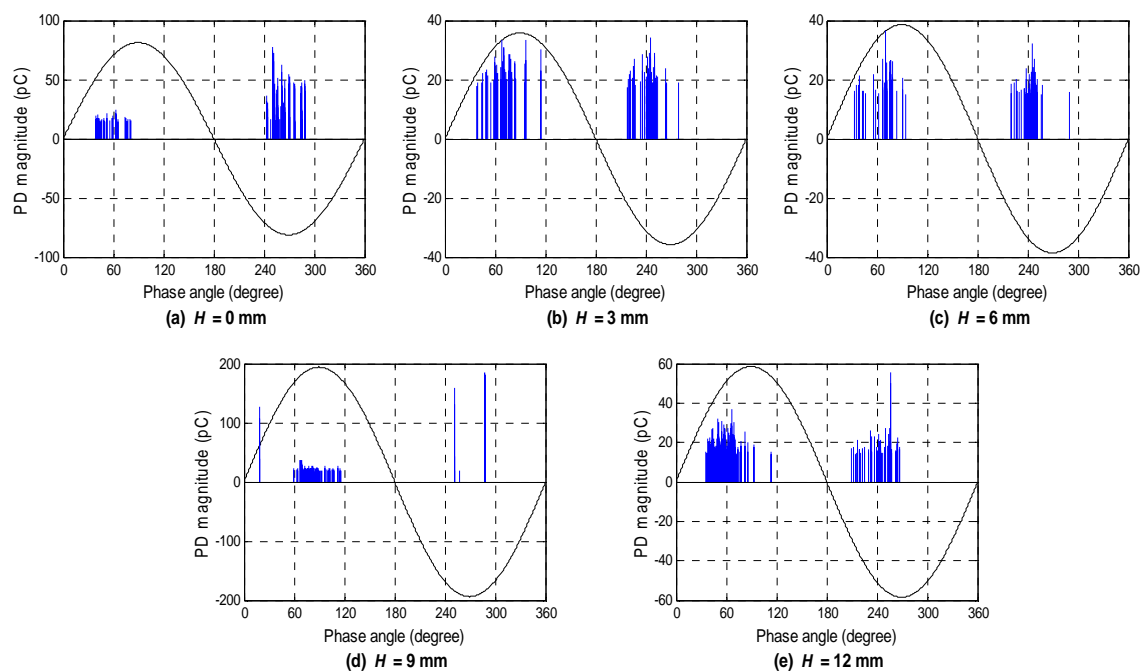


Fig. 6 Phase-resolved PD characteristics for particle of 3mm length at 2.5-bar SF<sub>6</sub> pressure

the total PD magnitude, although it is less than that obtained in the region between  $P = 1$  bar and  $P = 1.5$  bars.

A different pattern is found for particle of 3 mm length. As can be seen in Fig. 7(b), the drastic decreases in the total PD magnitude are obtained when the SF<sub>6</sub> pressure is increased from 1 bar to 2 bars, but only when the particle touches the electrodes. For the other particle positions, the changes in the total PD magnitude are still achieved, but with lower values. When the SF<sub>6</sub> pressure is increased from 2 bars to 3 bars, there is no significant decrease in the total PD magnitude at all.

TABLE II

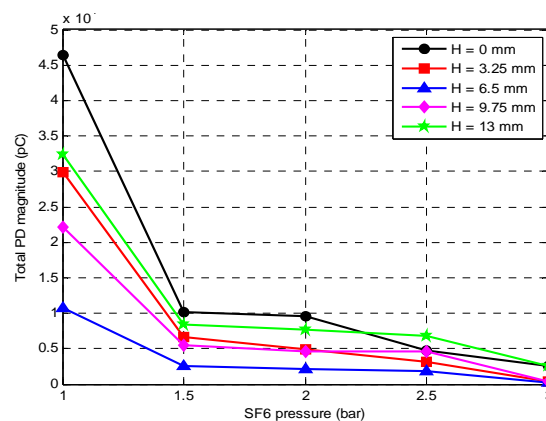
DISTRIBUTION OF PD MAGNITUDE IN EACH HALF-CYCLE EXPRESSED AS PERCENTAGES OF THE TOTAL PD MAGNITUDE FOR 3MM PARTICLE AT 2.5-BAR SF<sub>6</sub> PRESSURE

The value of $H$ (mm)	% PD magnitude	
	(+) half-cycle	(-) half-cycle
0	80.40426	19.59574
3	53.60337	46.39663
6	47.82054	52.17946
9	44.04525	55.95475
12	31.54143	68.45857

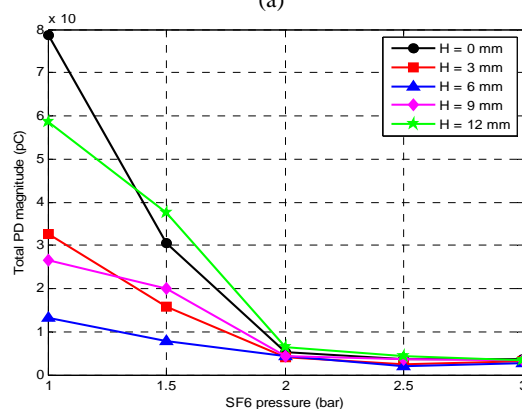
TABLE III

DISTRIBUTION OF PD MAGNITUDE IN EACH HALF-CYCLE EXPRESSED AS PERCENTAGES OF THE TOTAL PD MAGNITUDE FOR 3MM PARTICLE AT 3-BAR SF<sub>6</sub> PRESSURE

The value of $H$ (mm)	% PD magnitude	
	(+) half-cycle	(-) half-cycle
0	80.40426	19.59574
3	42.79155	57.20845
6	41.70835	58.29165
9	37.36678	62.63322
12	19.76517	80.23483



(a)



(b)

Fig. 7 The total PD magnitude for all particle lengths and positions as functions of the SF<sub>6</sub> pressure (a) Particle length  $L = 2$  mm (b) Particle length  $L = 3$  mm

#### IV. CONCLUSION

The PD measurements are carried out in a GIS model with metallic particle adhering to the spacer surface. The effects of particle length and position are investigated. The following findings are observed:

- (1) Longer metallic particle generates higher PD magnitudes.
- (2) When the particle is closer to the grounded electrode, a higher total PD magnitude occurs in the negative half-cycle. Conversely, PD occurs with a higher total magnitude in the positive half-cycle when the particle is closer to the HV electrode.
- (3) Total PD magnitude depends on SF<sub>6</sub> pressure but in a non linear manner.

#### REFERENCES

- [1] H. Anis, "Gas-insulated switchgear," in *High Voltage Engineering : Theory and Practice*, M. Khalifa, Ed. New York, NY: Marcel Dekker, Inc., 1990, pp. 243-273.
- [2] P. Bolin, "Gas-insulated substations," in *Electric Power Substations Engineering*, J.D. McDonald, Ed. Boca Raton, FL: Taylor & Francis Group, LLC, 2007, pp. 2.1-2.20.
- [3] H. S. Jain, "Gas-insulated sub-station / switchgear (GIS)," in *Handbook of Switchgears*, B.H.E. Limited, Ed. New York, NY: McGraw-Hill, 2007, pp. 5.1-5.26.
- [4] R. M. Radwan and A. M. Abou-Elyazied, "Effect of spacer's defects and conducting particles on the electric field distribution along their Surfaces in GIS," *IEEE Trans. Dielectr. Electr. Insul.*, vol. 14, pp. 1484-1491, December 2007.
- [5] Y. Khan, S. Okabe, J. Suehiro and M. Hara. "Particle initiated breakdown characteristics around spacer under lightning impulse voltage superimposed on pre-stressed DC", Institute of Electrical Engineers of Japan (IEEJ) *Trans. Fundamental and Materials*, Vol. 124, No.7, pp. 547-552, 2004.
- [6] Y. Khan, E.K. Lee, A. Oda, K.Sakai, Q. Zhang, S. Okabe, J. Suehiro and M. Hara., "Characteristics of corona and surface flashover triggered by free-conducting particles around simple shaped spacer under DC voltage in atmospheric air", *Proc. of 2001 Japan-Korea Joint Symposium on Electrical discharges and High Voltage Engineering (ED & HVE)*, Miyazaki, Japan. Vol.1, pp. 101-104, 1-2 November 2001.
- [7] A.A. Khan, Y.Khan, N.H.Malik and A. A. Al-Arainy, "Influence of spacer defects and adhered metal particles on electric field intensifications in GIS", *Journal of Basic Appl. Scientific Research*, J. Basic. Appl. Sci. Res., 2(8), pp. 7866-7875, August 2012.
- [8] N. Kanako, et al. "Particle size identification in GIS by ultra high speed measurement of partial discharge," *International Conference on Condition Monitoring and Diagnosis (CMD)*, pp. 443-447, 21-24 April 2008.
- [9] N. Hayakawa, et al. "Dependence of partial discharge characteristics at spacer surface on particle size in SF<sub>6</sub> gas insulated system," *International Conference on Condition Monitoring and Diagnosis (CMD)*, pp. 46-50, 21-24 April 2008.
- [10] Y. Negara, et al. "AC particle-triggered corona discharge in low pressure SF<sub>6</sub> gas," *IEEE Transactions on Dielectrics and Electrical Insulation*, Vol. 14, No. 1, pp. 91-100, February 2007.
- [11] CIGRE Working Group D1.33, "Guide for electrical partial discharge measurements in compliance to IEC 60270," *Technical Brochure*, Electra, pp. 61-67, December 2008.